

NRL Report 6253

# Ray Tracing in Rising and Falling Ducts

N. W. GUINARD, M. B. LAING, AND K. W. MORIN

*Wave Propagation Branch  
Electronics Division*

June 22, 1965

APPROVED FOR PUBLIC  
RELEASE - DISTRIBUTION  
UNLIMITED



U.S. NAVAL RESEARCH LABORATORY  
Washington, D.C.

## CONTENTS

Abstract	ii
Problem Status	ii
Authorization	ii
INTRODUCTION	1
RAY THEORY	4
LINEAR MODEL OF A VARYING ATMOSPHERE	5
RAY TRACING IN RISING AND FALLING DUCTS	7
LOSSES IN DUCTS WITH NONLINEAR BOUNDARIES	13
CONCLUSIONS	16
ACKNOWLEDGMENTS	17
REFERENCES	17
APPENDIX - Program Written in NELIAC Language for Ray Tracing in Rising and Falling Ducts	18

## ABSTRACT

In studying signal transmission beyond the horizon by elevated duct propagation, estimates are needed of the losses. These estimates can be made by application of ray tracing for models of longitudinally varying ducts. A program was written in the NELIAC language for producing ray trajectories in an atmosphere which is variable in two dimensions. The program was run in the NAREC digital computer, and the resulting plots of the ray paths are used to analyze certain of the loss mechanisms in elevated ducts. Changes of the acceptance angle, i.e., refractive index gradient at a fixed altitude can cause continued losses. Changes in duct geometry causes losses which are a function of the height slope distribution at the point of change. A third loss mechanism, that of scattering, is not handled in the present analysis, but it is pointed out that a discontinuous duct may approach the Booker and Gordon model for tropospheric scatter.

## PROBLEM STATUS

This is a final report on this phase of the problem; work on other phases is continuing.

## AUTHORIZATION

NRL Problem R07-02  
Project RR 008-01-41-5550

Manuscript submitted February 1, 1965.

## RAY TRACING IN RISING AND FALLING DUCTS

### INTRODUCTION

The phenomenon of signal trapping by elevated ducts was elaborately documented in the fourteen missions of the Tradewind III series flown by NRL between San Diego and Hawaii during a seven-week period in July and August 1960. Later analysis (1) uncovered the allied phenomenon of duct-scatter, by which an elevated duct may be loaded with signal energy from sources well below or well above the duct and, reciprocally, may scatter signal energy from the elevated duct to receivers located outside the duct boundaries. Figure 1 illustrates the common volumes in a duct-coupled communication link. Further studies of duct propagation phenomena have been concerned with the losses encountered in such a link both by changes in the refractivity profile and by the variation with altitude of the duct boundaries. It will be the purpose of this report to discuss both quantitatively and qualitatively the problem of duct loss from a ray standpoint and also to discuss certain cases which in the limit approach the conventional scatter theory.

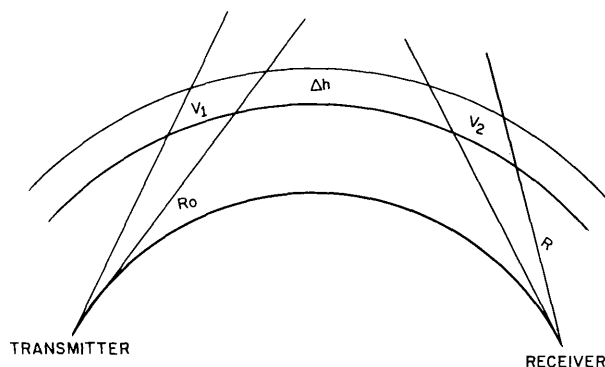


Fig. 1 - A duct-coupled communication link

The application of ray tracing to longitudinally varying ducts requires iteration of the ray equation in a model atmosphere which is variable in both range and elevation. From an inspection of the ray trajectories which result from such a calculation, losses may be estimated which at least qualitatively give insight into propagation losses in elevated ducts. The calculation of the ray trajectories was achieved by use of a medium-sized digital computer (NAREC) using the NELIAC language. In order to establish a background for the study of loss mechanisms certain fundamentals of ducting phenomena will be briefly described. A fuller treatment of this material will be found in Ref. 1.

Figure 2 shows a composite of data collected on mission 14 of the Tradewind III series. The curves labeled with Zebra time (third graph from the top) are profiles of the refractivity in N-units ( $(n - 1) \times 10^6$ , where  $n$  is the index of refraction). These profiles are notable since most possess at a definite altitude a severe discontinuity in the refractivity. It is well known that the effect of the curved earth can be represented by an artificial gradient of the refractivity of approximately 48 N-units per thousand feet. If this

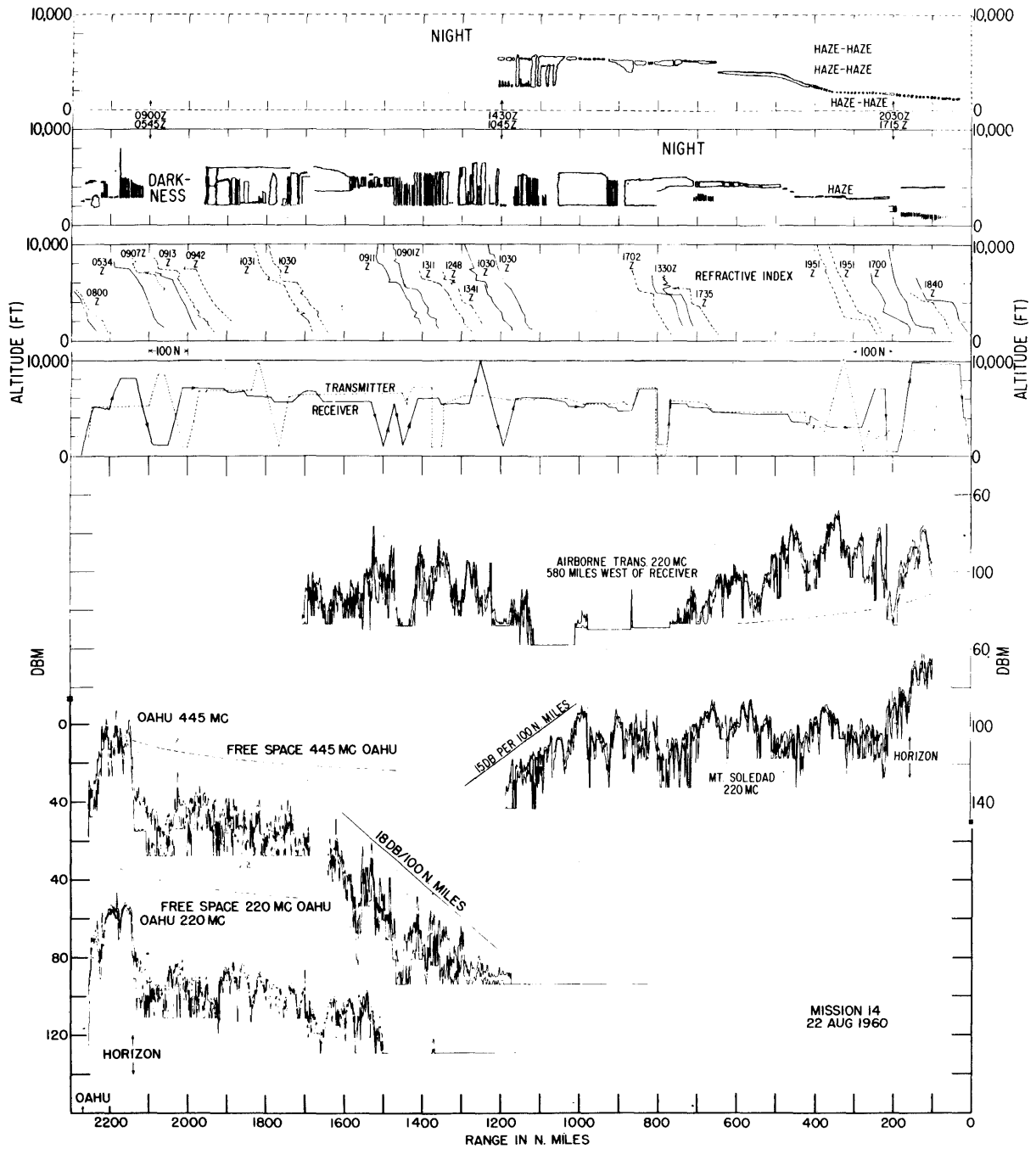


Fig. 2 - Data collected on mission 14 of the Tradewind III series

artificial gradient is exceeded by the actual atmospheric gradient, as in the figure, super-refraction results and the ray is bent toward the earth's surface. In the idealized profile in Fig. 3, the artificial gradient is shown as a dashed line. The triangular area bordered by this line defines the altitude range over which superrefraction occurs. Since the rays within these altitude boundaries are bent back to the earth's surface, energy can be trapped in this zone, and thus over the range in which the discontinuity in the profile exists a duct is formed. Such a duct can transport energy over the radio horizon to ranges well beyond those predicted by diffraction or scattering mechanisms.

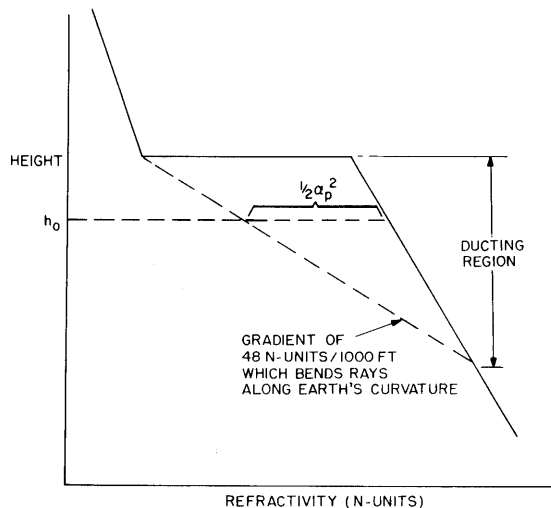


Fig. 3 - An idealized refractivity profile which is characteristic of an elevated duct

In particular, over the eastern portions of the tropical oceans there occurs with relatively high frequency a general descent of high-altitude dry air into regions where it meets low-level wet maritime air flowing toward the equator. Depending on the relative strengths of the air flows, at some altitude there exists a more or less turbulent interface between the wet air below and the dry air above. Since the index of refraction of wet air is higher than that of dry air, the characteristic discontinuity (N-break) exists at the interface and a ducting region is formed. Since the lower altitude boundary of the duct is above the surface of the earth, the duct previously described is termed "elevated." Both elevated and surface ducts exist everywhere over the earth's surface in the troposphere, although their geographic coverage and frequency of occurrence are more pronounced in tropical ocean regions.

The bending produced in the ducting region is not large. Consequently, only rays launched nearly parallel (within 1 degree) of the duct axis are trapped. Rays at greater angles may be bent from their initial path, producing "radio holes" (2); however, these are not the concern of the present report, although the techniques developed will find use in predicting such phenomena. The amount of bending produced by a given duct is determined by the penetration angle,  $\alpha_p$ , which may be computed graphically for a given launch altitude  $h_0$  as shown in Fig. 3. The penetration angle is the critical angle which divides a given pencil of rays launched within a ducting region into trapped and untrapped rays respectively, and is a function of altitude. At the upper and lower boundaries  $\alpha_p$  is zero and, therefore, rays launched outside this range of altitude will not be trapped regardless of angle of inclination at launch. The central angle of the trapped cone of rays is called the "acceptance angle,"  $\alpha$ , which is equal to  $2\alpha_p$ .

## RAY THEORY

The path or trajectory of electromagnetic radiation in a medium whose index of refraction is a function of position is determined by solving the Eikonal equation with suitable boundary conditions:

$$\nabla s = n . \quad (1)$$

This equation has been solved exactly given  $n$  as a continuous function of position (3). For a discontinuous index of refraction, with rays making small angles with the horizontal, in a two-dimensional atmosphere, the approximation

$$x = \int_{z_0}^z \frac{dz}{[(\beta_0^2/2) + n(z) - n(z_0)]^{1/2}} \quad (2)$$

is used (4), where  $x$  and  $z$  are the range and altitude of the ray respectively;  $\beta_0$  is the launch angle,  $n(z)$  and  $n(z_0)$  are the index of refraction of the atmosphere at heights  $z$  and  $z_0$ . In order to produce a working relationship which can be used to generate a ray family in a piecewise linear medium, Eq. (2) must be rewritten in terms of the refractivity and also with respect to a flat earth. Omitting the algebra of rewriting Eq. (2), the following form will be used:

$$x = \pm 0.1339 \sum_{n=1}^N \frac{\Delta z}{[(\beta_0^2/2) + 0.048 \Delta z - \Delta N_n]^{1/2}} . \quad (3)$$

In Eq. (3), the atmosphere has been subdivided into  $N$  equal altitude segments  $\Delta z$  feet in height. The gradient of the refractivity in each segment is assumed constant, and  $\Delta N_n$  is the total change of refractivity in the  $n$ th segment. The angle  $\beta_0$  is in milliradians, and the range  $x$  is in miles. To develop a ray trajectory, Eq. (3) is solved for each height increment in order, generating points

$$\left( \sum_k \Delta k, k \Delta z \right),$$

where  $k$  is an integer running from 1 to  $N$ . The smooth curve connecting the points is the desired trajectory.

For positive launch angles in a nonsuperrefractive atmosphere the ray picture may be determined by varying the launch angle in Eq. (3) through the desired beamwidth. However, for negatively launched rays or superrefractive atmosphere the ray trajectory becomes parallel to the flat earth and Eq. (3) breaks down, yielding an infinite or imaginary result. Such a point, using the ray optics concept, is termed a "caustic." To trace through a caustic, Wong (3) has used the fact that a ray in a medium which is homogeneous is bent parabolically; thus in an altitude slice sufficiently small to be considered homogeneous,

$$z = \frac{x^2}{2a} + \beta_n x + z_0 \quad (4)$$

where  $\beta_n$  is the ray inclination and  $a$  is the earth radius.

If the value of the inclination angle is known at a point  $(x_1, z_1)$  close to the caustic, Eq. (4) yields a relationship between the coordinates of the caustic  $(x_c, z_c)$ . To determine the approximate height of the caustic,  $z_c$ , the following iteration is used. If  $(x_1, z_1)$  is

chosen as the last real point before the breakdown of Eq. (3), the altitude segment including the caustic and  $(x_1, z_1)$  is subdivided into smaller increments, say,  $\Delta z/10$  and the calculation of the trajectory continued until the ray equation fails again. This point  $(x_1 + \Delta x, z_1 + (\Delta z/10))$ , provides a more accurate approximation of  $z_c$ . The process is continued until

$$z_1 + \frac{\Delta z}{10} + \frac{\Delta z}{100} + \dots \approx z_c \quad (5)$$

to the desired accuracy. At this point

$$\Delta x = -2 a \beta_n, \quad \beta_n = \pm [(\beta_0^2/2) + 0.048 \Delta z' - \Delta N']^{1/2} \quad (6)$$

where  $\beta$  is the last computed angle of inclination and  $\Delta x$  is the range segment from the last computed point to the caustic. The trajectory is returned to the range of Eq. (3) by assuming symmetry of the trace on either side of the caustic. The sign of  $\Delta z$  is reversed and the calculation continued. Figure 4 shows the result of this technique applied to a profile similar to Fig. 3 in a horizontally stratified atmosphere.

#### LINEAR MODEL OF A VARYING ATMOSPHERE

In order to model a varying atmosphere it is necessary to make an assumption concerning the behavior of the profile which is intermediate between two known profiles. For those conditions where the upper portion of the ducting region is formed at the interface of two extensive air masses as in the tradewinds region it is natural to assume the continuity of the duct. The functional form of the variation of refractivity and height with range along the boundary is less certain. In the present model it was assumed that the variation of both refractivity and height with range is linear. Furthermore, it is assumed that the variation of refractivity with height is assumed to be piecewise linear. These assumptions form the basis for Fig. 5. The refractivity,  $N$ , is assumed to be linear along the upper boundary of the model, the upper interface boundary, the lower interface boundary, and the flat earth. The height of the duct axis is assumed linear with range. In the example shown the preferred linear directions are obvious from elementary considerations. However, in more complicated situations, where the profiles have unequal numbers of segments or a ducting refractivity profile degenerates to a linear profile, more complicated assumptions are required.

In the model shown in Fig. 5, three zones are defined: the atmosphere above the interface, the atmosphere below the interface, and the interface itself. In each zone an expression may be determined to extrapolate  $N$  at any point in the zone from its value at the known points on the profile at ranges  $x_0$  and  $x_1$  respectively.

To find such a relationship for zone II, the variation of refractivity along the upper boundary  $R_3$  is given by

$$N_u = \frac{N'_3 - N_3}{X_m} x + N_3 \quad (7)$$

where  $X_m$  is the distance between known profiles. Likewise, along the lower boundary,

$$N_l = \frac{N'_2 - N_2}{X_m} x + N_2 \quad (8)$$

At some altitude  $z$  lying between the interface boundaries,

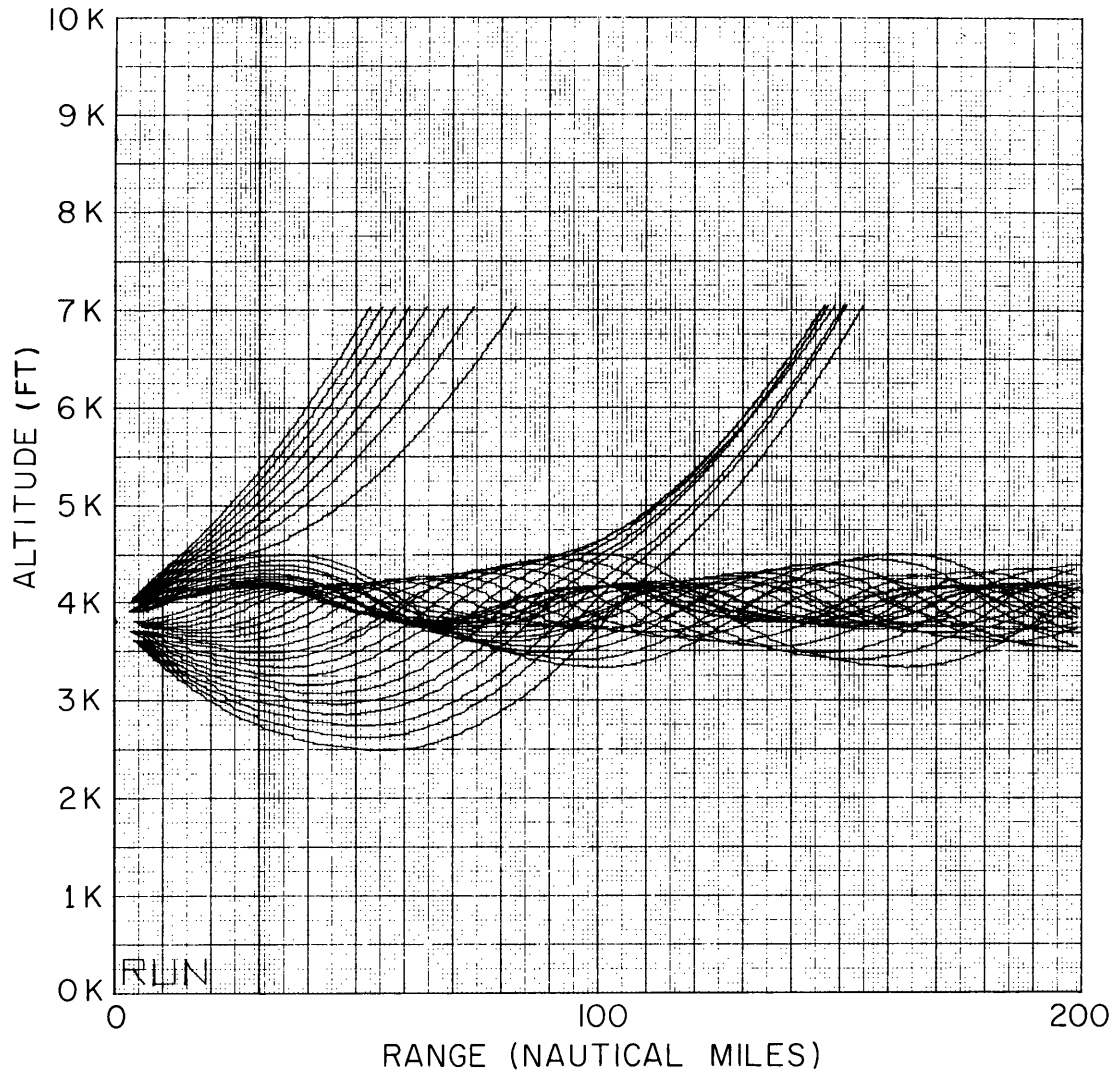


Fig. 4 - Family of ray paths calculated using a horizontally stratified atmosphere

$$N = \frac{z - z_{\ell}}{z_u - z_{\ell}} (N_u - N_{\ell}) + N_{\ell} \quad (9)$$

where  $z_u$  and  $z_{\ell}$  are the variable heights of the upper and lower boundaries given by

$$z_u = \frac{z'_3 - z_3}{X_m} x + z_3$$

$$z_{\ell} = \frac{z'_2 - z_2}{X_m} x + z_2$$

The difference in the refractivity at heights  $z_1$  and  $z_2$  which lie between  $z_u$  and  $z_{\ell}$  at range  $x$  becomes

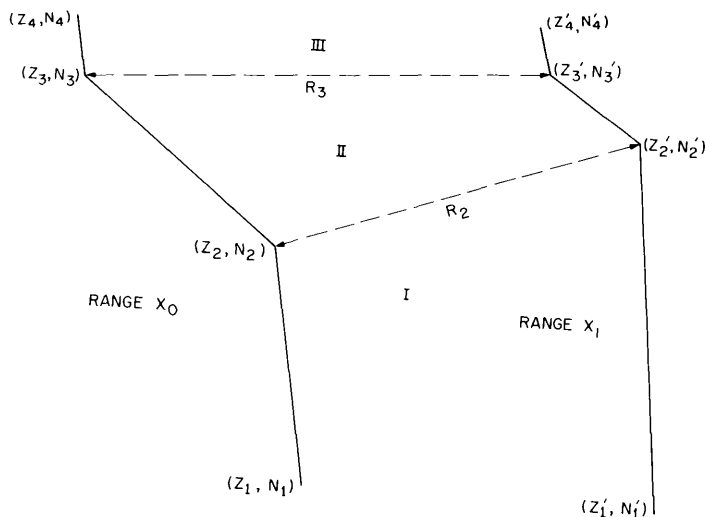


Fig. 5 - Two refractivity profiles illustrating a model in which the variation of refractivity is linear with range and piecewise linear with height

$$\Delta N = \frac{N_u - N_\ell}{z_u - z_\ell} \Delta z . \tag{10}$$

The variation of refractivity in other zones may be obtained from Eq. (17) by substitution of their respective boundary lines.

RAY TRACING IN RISING AND FALLING DUCTS

A complete set of equations which will allow the generation of a ray family in an atmosphere varying with range and elevation include:

$$x = 0.1339 \sum_{n=1}^N \frac{\Delta z}{[(\beta_0^2/2) + 0.048 \Delta z + \Delta N_n]^{1/2}} \tag{11a}$$

$$N_u = \frac{N'_3 - N_3}{X_m} x + N_3 \tag{11b}$$

$$N_\ell = \frac{N'_2 - N_2}{X_m} x + N_2 \tag{11c}$$

$$z_u = \frac{z'_3 - z_3}{X_m} x + z_3 \tag{11d}$$

$$z_\ell = \frac{z'_2 - z_2}{X_m} x + z_2 \tag{11e}$$

$$\Delta N = \frac{N_u - N_l}{z_u - z_l} \Delta z \quad (11f)$$

$$z \approx z_0, \quad \Delta x = -2a\beta_n \quad (11g)$$

$$\beta_n = \pm [(\beta_0^2/2) + 0.048 \Delta z - \Delta N_n]^{1/2}. \quad (11h)$$

Starting at launch  $(x_0, z_0)$ , Eq. (11a) is used with the known profile at  $x_0$  to compute the range increment  $\Delta x$  for the first height increment  $\Delta z$ . The range  $(x_0 + \Delta x)$  is used with Eqs. (11b) through (11f) to determine  $\Delta N$ . This value of  $\Delta N$  is used with Eq. (11a) to determine  $\Delta x'$ . The process is reiterated until consecutive values of the range increment differ by a prescribed amount, say, 1 percent. After  $\beta_n$  is determined from Eq. (11h),  $\beta_n$  and the last computed values of  $\Delta x$  and  $\Delta N$  are used with Eq. (11a) to determine the next range increment by the same method. Near a caustic, Eq. (11g) is substituted for Eq. (11a) and the iterative process repeated.

Using this scheme with bookkeeping operations on height, angle and zone, a program was written in NELIAC language and executed in the NAREC computer. This program is reproduced in the appendix. Table 1 of the NELIAC program contains the nomenclature, definitions, and range of the input variables. The output of this program is a 3/4-inch seven-level punched paper tape suitable for off-line plotting. The tape lists the coordinates  $(x + \Delta x, h \pm \Delta h)$  of the ray trajectory.

Table 1  
Effect of Duct Slope on the Symmetry of the Penetration Angles

Fig. No.	Duct Slope	$\alpha_p^+$ (mrad)	$\alpha_p^-$ (mrad)	$\alpha_c$ (mrad)
4	0	6	-6	0
6	$0.189 \times 10^{-3}$	6.3	-5.9	+0.2
7	$-0.189 \times 10^{-3}$	5.8	-6.2	-0.2
8	$1.89 \times 10^{-3}$	8.2	-4.4	+1.9
9	$-1.89 \times 10^{-3}$	4.3	-8.2	-1.95

Figure 4 and Figs. 6 through 11 are ray traces produced by this program. Figures 6 through 9 are ray traces for various duct axis inclinations. Figure 4 is a ray plot of propagation in a stratified atmosphere whose refractivity profile is similar to that in Fig. 3. The concept of the acceptance angle associated with a superrefractive atmosphere is strikingly shown in this figure. A transmitter of power  $P_0$  at the launch point shown would encounter a coupling loss equal to

$$L = 10 \log \frac{\alpha(z_0)}{2b}, \quad 2b \geq \alpha(z_0) \quad (12)$$

where  $b$  is the half-power beamwidth of the transmitting antenna and  $\alpha(z_0)$  is the acceptance angle at the launch altitude  $z_0$ .

Of greater interest than Fig. 4 is the situation in which the atmosphere varies with range. Figures 6 through 9 are examples of the ray trajectories produced by geometrically

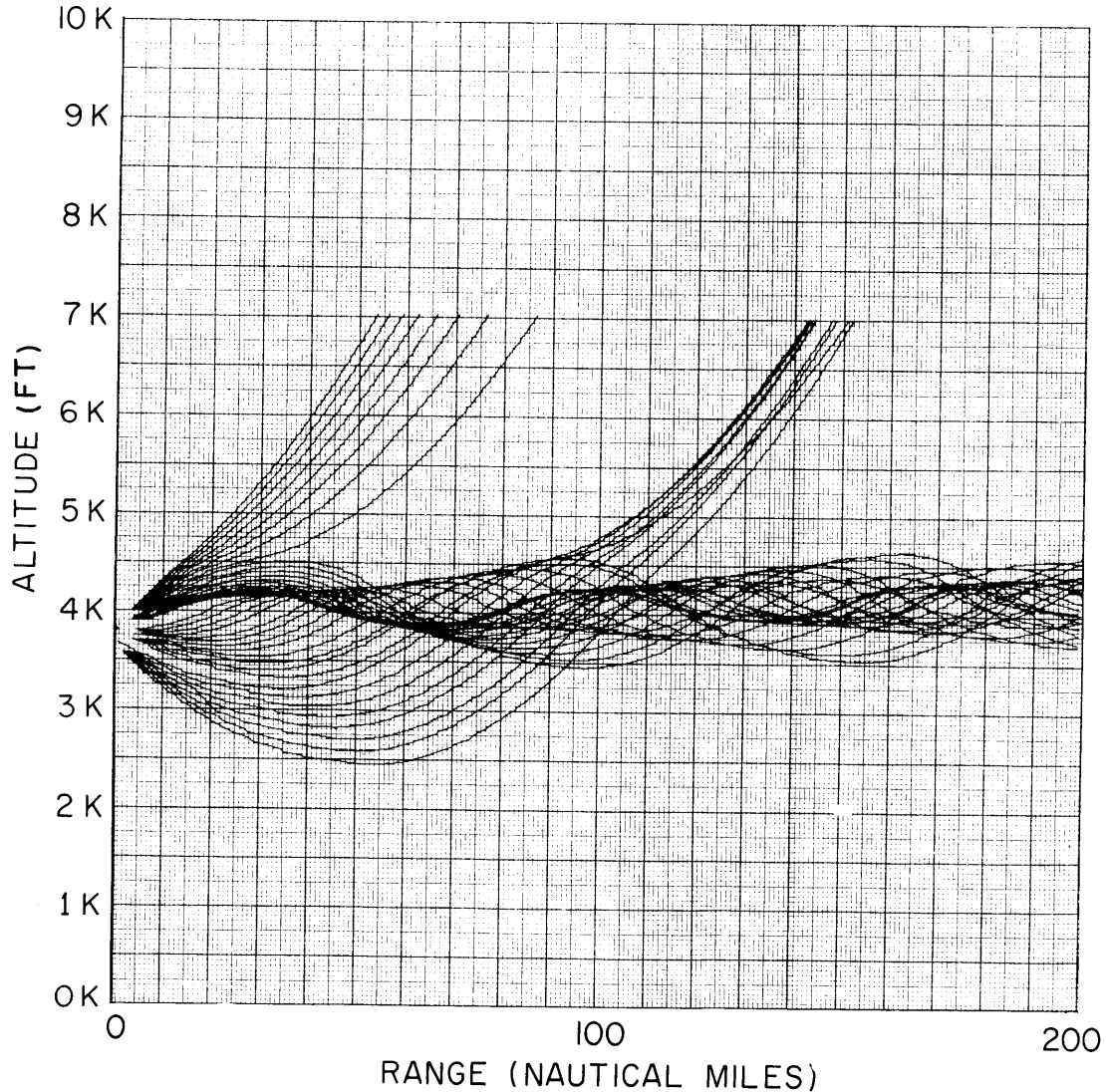


Fig. 6 - Family of ray paths calculated for a 500-ft-thick interface with a slope of  $0.189 \times 10^{-3}$ , a gradient in the interface of  $-0.1$  N-units per ft, and a gradient above and below the interface of  $-0.01$  N-units per ft

varying ducts. In all cases, the profile used was trilinear with a 500-ft duct thickness whose gradient was  $-0.1$  N units per ft. The gradient above and below the duct was  $-0.01$  N units per ft. By varying the height of the duct as a function of range the rising and falling duct models were generated. The major effect of the tilting of the duct axes is to disturb the symmetry of the penetration angles without, however, altering the acceptance angle. Table 1 demonstrates this result for various duct slopes. This data was taken from ray plots whose angle quantization was  $0.1$  mrad, which accounts for the numerical discrepancies between the duct slope and symmetry angle  $\alpha_c$ . The plots shown are quantized in  $0.5$ -mrad steps. The symmetry angle  $\alpha_c$  is defined by

$$\alpha_c = \frac{\alpha_p^+ + \alpha_p^-}{2} \quad (13)$$

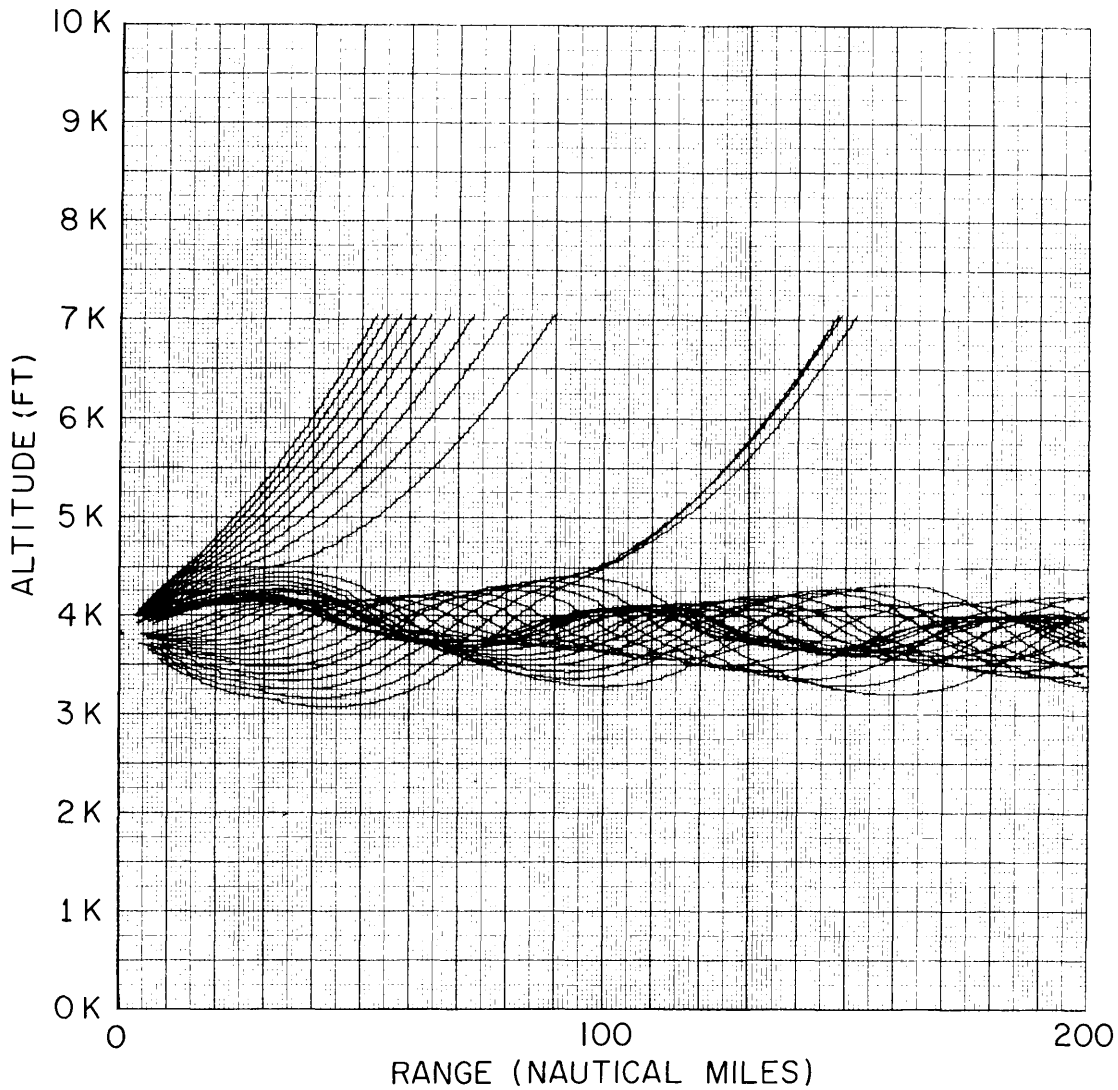


Fig. 7 - Family of ray paths calculated for a 500-ft-thick interface with a slope of  $-0.189 \times 10^{-3}$ , a gradient in the interface of  $-0.1$  N-units per ft, and a gradient above and below the interface of  $-0.01$  N-units per ft

Consequently, the effect of duct slope is to rotate the penetration angles from  $\pm\alpha_p$  for a stratified ducting atmosphere to  $\pm\alpha_p + \tan^{-1}s$ , where  $s$  is the slope of the duct axis. The coupling loss (Eq. (12)) is unchanged. After loading, further changes in the duct axis tilt will result in the loss of those rays whose instantaneous slope exceeds that permitted by the penetration angles.

To formalize this result, a ray family may be represented at a range  $x$  by vectors of infinitesimal length with slopes distributed primarily within the tangents of the penetration angles. Such a vector may be represented by

$$\mathbf{u} = \mathbf{v} e^{-j \tan^{-1} s}. \quad (14)$$

Collectively the ray family at  $x$  may be represented by a two-dimensional scalar density function which yields the number of rays at a given height  $z$  with slope  $s$ . This function

is known as the height slope density function. The integral of this function over all slopes is the height gain function which is measurable. Now, let  $P(z_0, s)$  be the height slope density function generated by a transmitter located at  $(z_0, x_0)$ . Then

$$N = \int_{-\infty}^{\infty} P(z_0, s) ds \tag{15}$$

where  $N$  is the total number of rays launched. The duct accepts a portion of rays equal to

$$N_T = \int_{\tan \alpha_p^-(z_0)}^{\tan \alpha_p^+(z_0)} P(z_0, s) ds, \quad z_1 \leq z_0 \leq z_2 \tag{16}$$

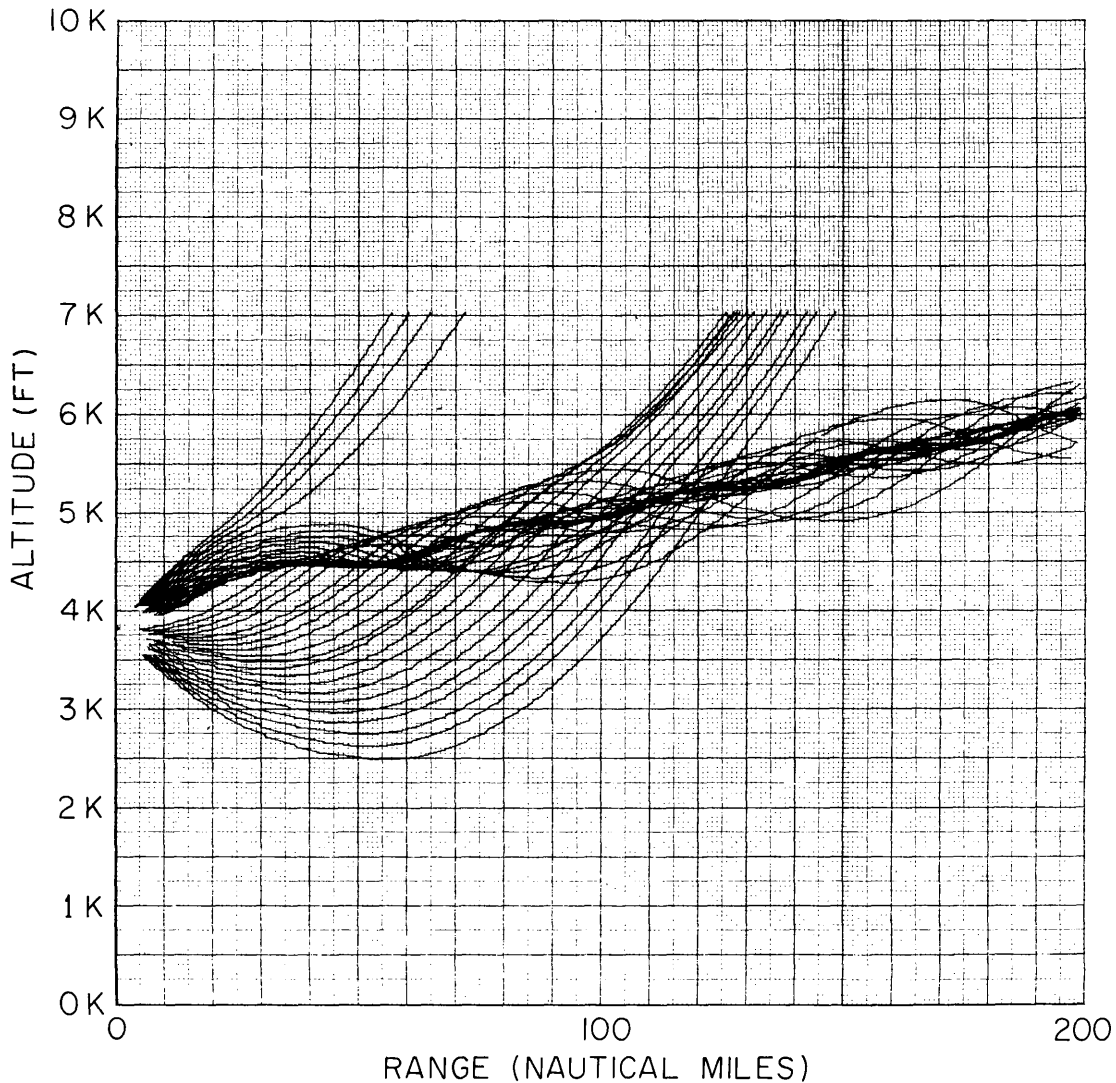


Fig. 8 - Family of ray paths calculated for a 500-ft-thick interface with a slope of  $1.89 \times 10^{-3}$ , a gradient in the interface of  $-0.1$  N-units per ft, and a gradient above and below the interface of  $-0.01$  N-units per ft

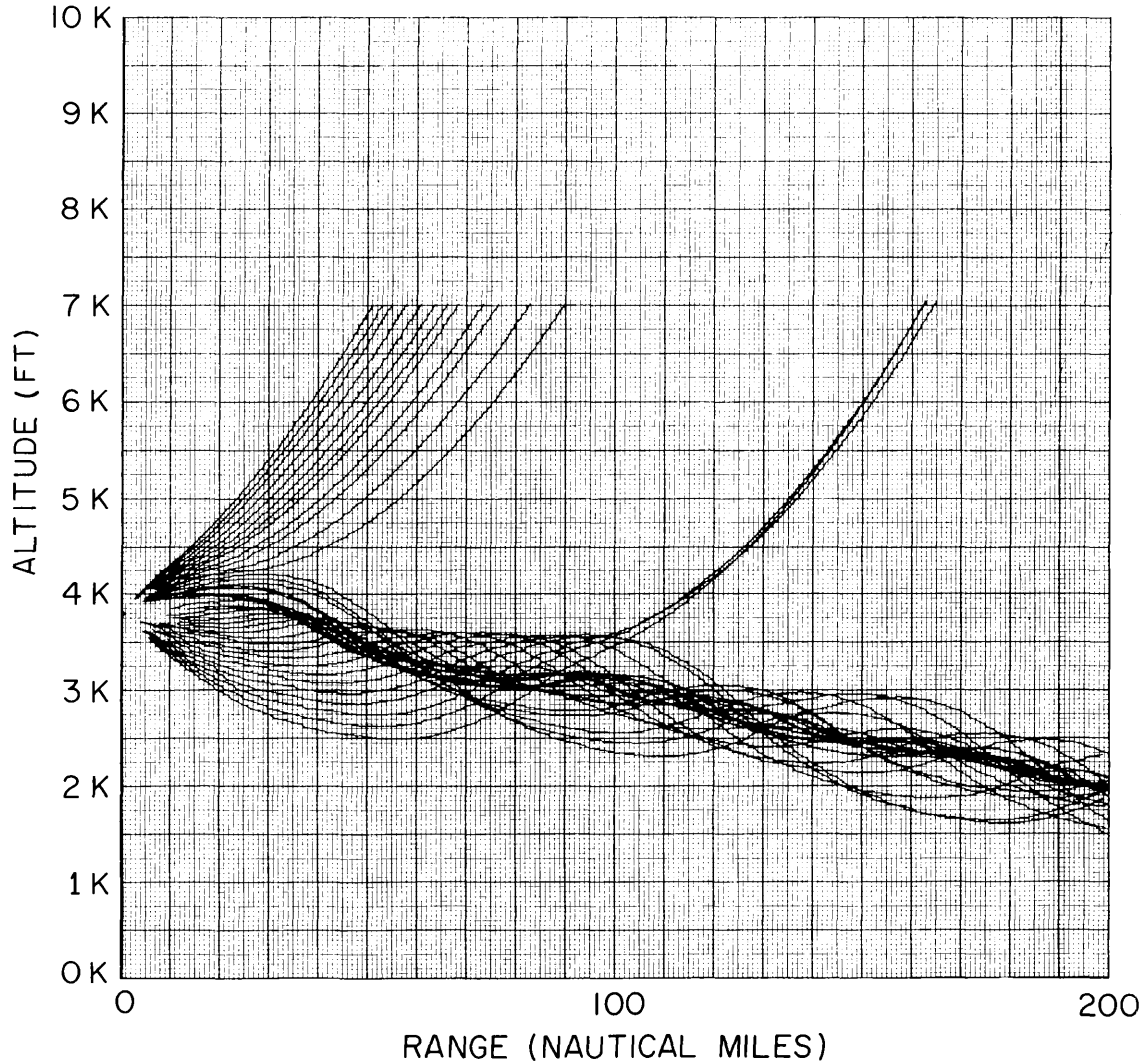


Fig. 9 - Family of ray paths calculated for a 500-ft-thick interface with a slope of  $-1.89 \times 10^{-3}$ , a gradient in the interface of  $-0.1$  N-units per ft, and a gradient above and below the interface of  $-0.01$  N-units per ft

where  $N_T$  is the number of trapped rays and  $z_1$  and  $z_2$  are the altitudes of the duct boundaries. If at some range  $x$ , the duct axis changes its inclination by an amount  $\theta$ , the number of rays which will continue trapped is given by

$$N'_T = \int_{z_1}^{z_2} \int_{\tan(\alpha_p^-(z)+\theta)}^{\tan(\alpha_p^+(z)+\theta)} Q(z, s) \, ds \, dz \quad (17)$$

where  $Q(z, s)$  is the height slope density function in the duct and is defined by

$$N_T = \int_{z_1}^{z_2} \int_{-\infty}^{\infty} Q(z, s) \, ds \, dz \quad (18)$$

The loss (gain) produced by the transition becomes

$$L_T = 10 \log \frac{N'_T}{N_T} . \quad (19)$$

An illustration of this process is shown in Fig. 10. The duct axis is steeply inclined at a 2500 ft per hundred mile slope and then descends at the same rate. Inspection of this figure will show that the rays which remain trapped do so because of their height and slope at the transition rather than their initial launch angle. This result allows a quantitative evaluation of the loss involved in axis variations from the geometry (derived from cloud heights) and refractivity profiles, since a two-dimensional Gaussian height slope function may be assumed with good justification.

An allied problem in duct loss calculation is that of a duct which varies in acceptance angle at constant slope. This problem is simply handled, since the result is a continual decrease of width of the height slope function. Figure 11 is a ray plot of this situation which shows a linear variation from  $\alpha_1$  at range zero to  $\alpha_2$  at range 400 miles. The continual loss of power gives rise to a loss rate which is given by

$$\begin{aligned} \text{power loss rate} &= \frac{10}{R} \log \frac{\alpha_2}{\alpha_1} \text{ db/mile,} & \alpha_2 < \alpha_1 \\ &= 0, & \alpha_2 \geq \alpha_1 . \end{aligned} \quad (20)$$

From ray theory, therefore, two loss mechanisms are apparent, the loss produced by rotation of the acceptance cone and the loss produced by a decrease in the acceptance angle. These, however, are not all inclusive. A third mechanism, scattering loss due to irregularities in index of refraction between the duct boundaries must be approached from statistical forms of analysis. A Monte Carlo approach to this problem is presently underway.

#### LOSSES IN DUCTS WITH NONLINEAR BOUNDARIES

Meteorological investigations of duct structure carried on in the Bahamas and the Pacific Tradewinds regions by NRL have indicated that the interface between wet and dry air which produces the characteristic discontinuity in refractivity (N-break) undulates with periods of several miles. This continuous movement of the duct axis should produce a db/mile loss rate proportional to the rate of change of slope as well as the rate of change of acceptance angle. An attempt to handle both parameters in a closed form has proved intractable. However, if the acceptance angle is assumed constant, then the loss between two points in the undulating duct where the slopes are  $s_1$  and  $s_2$  respectively should be approximately

$$L_u \approx \frac{(s_2 - s_1)}{\alpha} . \quad (21)$$

For a continuously varying duct the loss rate becomes

$$\frac{dL}{dx} = \frac{1}{\alpha} \frac{ds}{dx} . \quad (22)$$

Assuming that the height of the duct axis is given by

$$h = A \sin \frac{2\pi}{\lambda} x \quad (23)$$

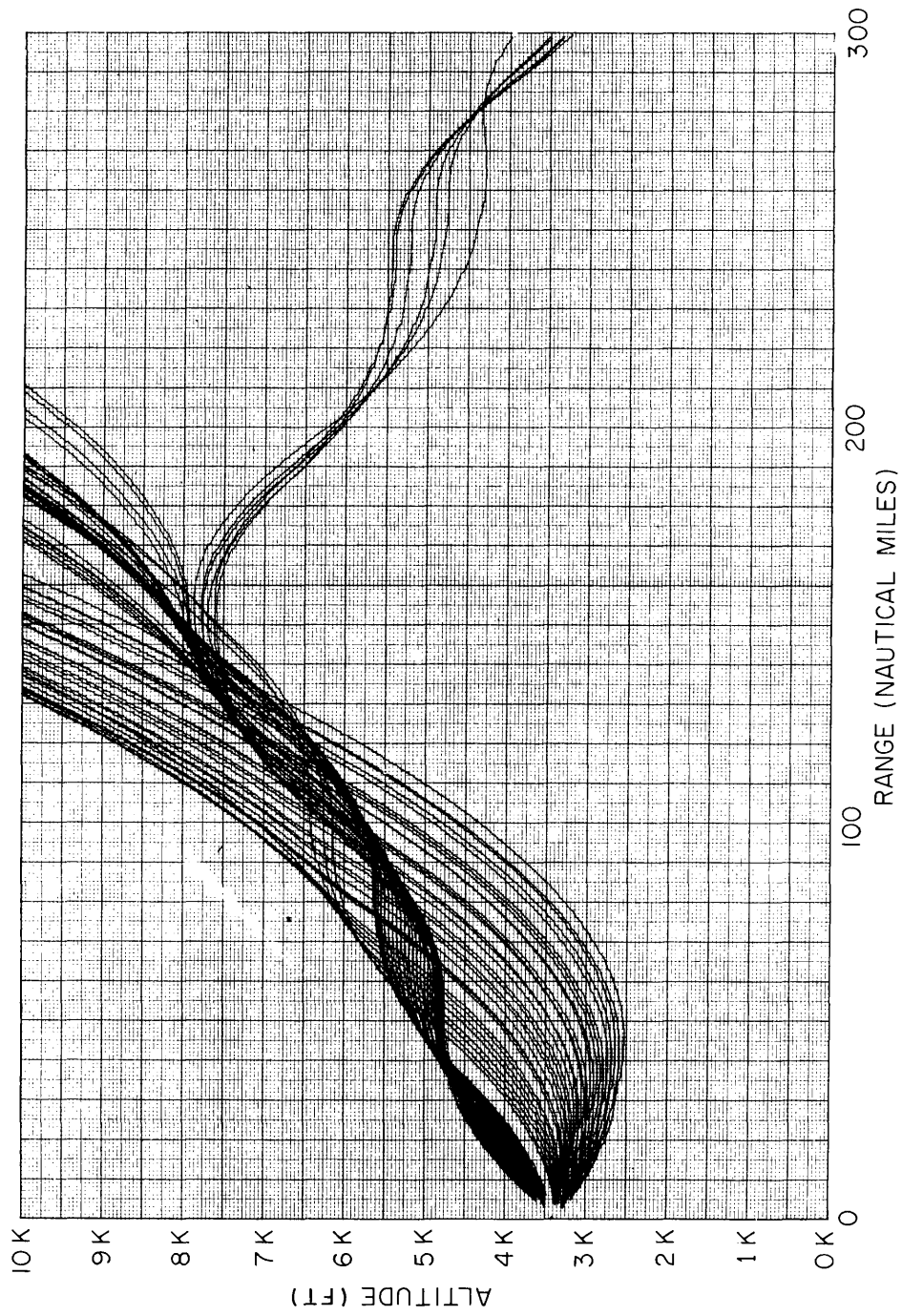


Fig. 10 - Family of ray paths calculated for a 500-ft-thick interface with a slope which changes at 150 miles from  $4.17 \times 10^{-3}$  to  $-4.17 \times 10^{-3}$ , a gradient in the interface of -0.1 N-units per ft, and a gradient above and below the interface of -0.01 N-units per ft

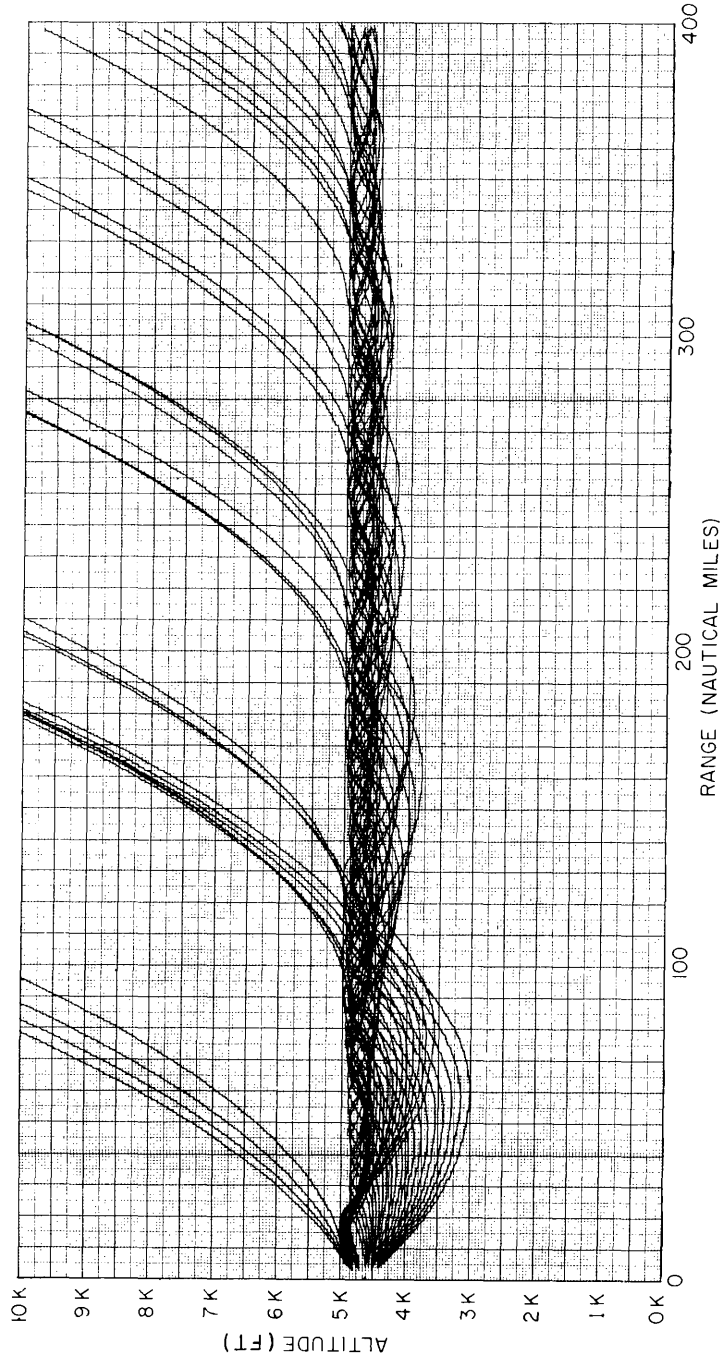


Fig. 11 - Family of ray paths calculated for a 500-ft-thick horizontal interface, a gradient in the interface which changes linearly from 0.2 N-units per ft at zero range to 0.05 N-units per ft at 400 miles, and a gradient above and below the interface of 0.01 N-units per ft

where  $A$  is the excursion and  $\ell$  the scale length. Then the loss rate becomes

$$\text{power loss rate} = -\frac{40}{\ell} \log \left( 1 - \frac{2\pi A}{\ell \alpha} \right) \text{ db/mi}, \quad 2\pi A < \ell \alpha. \quad (24)$$

The condition associated with Eq. (24) sets a criterion for the maximum excursion of duct altitude. This criterion is, however, overly strict, since the rotation of the acceptance was used as a basis rather than the more exact height slope function. The importance of the statement is that there exists a critical excursion above which the rays view the duct as discontinuous rather than undulating.

Under these circumstances, it is advisable to consider the situation of a duct of given  $\alpha$ ,  $\alpha_p^+$ ,  $\alpha_p^-$ , and  $z$ , which is broken at finite intervals with homogeneous atmosphere existing between the breaks. A pencil of rays which enters a break after being contained by a duct segment is bent with respect to a flat earth in the homogeneous atmosphere by an amount  $\theta$  given by  $d/a$  where  $a$  is the earth radius and  $d$  is the distance traveled by the pencil. The penetration angles then become  $\alpha_p^+ + \theta$  and  $\alpha_p^- + \theta$ . If at some distance  $d_1$  there exists another duct segment with similar characteristics, energy will be re-trapped for those rays whose slopes satisfy the condition

$$\alpha_p^- + \theta \leq \tan^{-1} s \leq \alpha_p'^+ \quad (25)$$

where  $\alpha_p'^+$  is the upper penetration angle of the second segment. The loss encountered in crossing the homogeneous area becomes

$$L = \frac{a \alpha_p'^+ - a \alpha_p^- - d_1}{a \alpha} \quad (26)$$

Within the limits of Eq. (25), Eq. (26) may be used to determine the loss for a given duct segment spacing or the spacing for a given loss.

The discontinuous duct model has wider application than might be immediately apparent. The moisture boundary associated with cloud structures produce at cloud altitude a severe N-break which produces a superrefractive condition. Thus propagation through scattered clouds may well be viewed from the standpoint of the discontinuous ducting model. For a given discontinuity in the refractivity at cloud tops and the mean spacing between clouds, estimates of propagation losses in such a medium can be obtained from Eq. (26). In addition, the correspondence between the discontinuous ducting model and the Booker and Gordon "blobby vacuum" model is striking. In the large scale limit, the acceptance angle and duct segment spacing may well become analogous to the scatter coefficient and scale of the latter model. However, further study along these lines is required to ferret out the desired relationship.

## CONCLUSIONS

By ray tracing, using a variable-parameter computer program, certain mechanisms of duct losses have been deduced. These involve primarily the loss of signal produced by variations of duct axis slope which rotate the acceptance cone without altering the acceptance angle and by the change in acceptance angle at constant slope. A formula which combines both of these mechanisms was unattainable. It was shown in Fig. 11 that the duct loss at a slope discontinuity was a function of the height slope density function at the point rather than the acceptance cone, although the latter was used as an approximation of the exact situation. Using these two mechanisms, two models, namely, the undulating and discontinuous ducting atmospheres, were analyzed and quantitative expressions for duct losses in these situations were achieved. The results in the latter model seem

to indicate a limiting case of the Booker and Gordon model for tropospheric scatter, and work will continue to expand this notion. In general, it is felt that the use of the acceptance angle concept of duct propagation allows both intuitive insight into propagation processes in elevated ducts and in the limit should allow the integration of ray theoretic principles with those of scatter theory to produce a consistent picture of tropospheric propagation.

#### ACKNOWLEDGMENTS

Assistance in the production of this report is gratefully acknowledged, in particular, to F. C. Macdonald and W. S. Ament for profitable suggestions in the course of research; also, assistance in developing the ray plots used herein is acknowledged to A. B. Bligh and the NRL Computer Facility.

#### REFERENCES

1. Guinard, N.W., Ransone, J., Randall, D., Purves, C., and Watkins, P., "Propagation Through an Elevated Duct: Tradewinds III," IEEE Trans. AP-12:479 (July 1964)
2. Wong, M.S., "Refraction Anomalies in Airborne Propagation," Proc. IRE 46:1628 (Sept. 1958)
3. Wong, M.S., "Ray-Tracing Picture of Radiowave Propagation in an Arbitrary Atmosphere," Wright Air Development Center, Air Force Technical Report 6631, July 1951
4. Kerr, D.E., "Propagation of Short Radio Waves," New York:McGraw-Hill, MIT Radiation Laboratory Series, Vol. 13, 1951

Appendix

PROGRAM WRITTEN IN NELIAC LANGUAGE FOR RAY TRACING  
IN RISING AND FALLING DUCTS

```

5
(:PAGE F4985 - 100 N -1)
RAY TRACING, #3500, ..
5
PRINT H (3) = 0000.00*0,
LEEWAY = {#0023}.
NO1,
NOO,
N11,
PRNTDH = 000.000*0,
B (3) = 000.000*0,
XPRIME (3) = 000.000*0,
DELTAN (3) = 000.000*0,
RANGE (3) = 0000.000*0,
PRINT TEST,
XMAX = {#001d}.
HMAX = {#001e}.
YCOOD,
XCOD,
INCR = 50.0,

(:PAGE F4985-100n-2)
XC.
YC.
STOP = #F0F082F0F082,
N10,

```

```

DELTAX.
H11,
H10,
H01,
LAUNCH ALT = {#0022},
LA = {#0021}.
BMAX = {#001B}.
DELTAB = {#001F}.
BMIN = {#001C}.
TC = {#0020},
DELTAH = {#0024}.
X = {#0054}.
A = {#0001}.
H00,

(:PAGE F4985-100n-3)
HTABLES (100) = #00e9,
NTABLES (100) = #00b7,
BK.
IORD = 01,
DELTAH MIN.
H0 TEST.
H1 TEST.
TS.
TS1.
COUNT = 1,
BK TEST (2).

```

BEGIN = #2f,  
 END = #3f,  
 END RUN = #3d,  
 BKM = 0.01:

SERIES START:

, COORDINATES, TRUESTART: X MAX - LEE WAY → X MAX.  
 NEW RAY..

5;

(:PAGE F4985-100n-4)

, XCOORDINATES: {I = 0(50)XCOORD {FLOAT PUNCH (XC, YC;),  
 XC + INCR → XC}}

, YCOORDINATES: {I = 0(50)YCOORD {FLOAT PUNCH (XC, YC;),  
 YC + INCR → YC}}

, COORDINATES: {PRINT TEST ≠ 0;;

FL TO FX (HMAX; YCOORD), FL TO FX (XMAX; XCOORD),  
 XCOORD \* 10 → XCOORD, TF, BEGIN #24, 0 #90,  
 XCOORDINATES, YCOORDINATES, -INCR → INCR, XCOORDINATES,  
 YCOORDINATES;}

, TF: {I = 0(1)199 {0 #71; 0 #90}} ..

5;

(:PAGE F4985-100n-5)

NEWRAY: LEE WAY → DELTA H MIN, 0 → J, ZERO LOCATIONS, PRINT TEST = 0:

END #24, 0 #90, TF, BEGIN #24, 0 #90;

, {<>;<<|||PH|||DELTA|H|||BETA|||X|PRIME||DELTA|N||RANGE  
 ||>>>};

BMAX → B, LAUNCH ALT → L, BMAX ≥ 0:

|IORD| → IORD, | DELTAH[1] | → DELTAH → DELTA H[1], |DELTA H MIN| →  
 DELTA H MIN;

```

#ffff ff ffff ff → IORD, - | DELTAH[1] | → DELTAH → DELTA H [1],
- |DELTA H MIN| → DELTA H MIN;
LA → PRINTH, |DELTA H| * BKM → BKTEST, 4 → J, ZERO LOCATIONS,
PRINT OR PUNCH, DELTA H[1] → DELTAH,
BK TEST → BK TEST [1],

```

```
RAY + 1 → RAY, PRINTEROK = 0:
```

```
RAYCOUNTER(RAY);;
```

```
SET UP TABLES..
```

```
5;
```

```
(:PAGE F4985-100n-6)
```

```
SET UP TABLES: I = 0(1) TC {ENTRY:, START COMPUTE, ENTRY. RE:}
```

```

,START COMPUTE: {STCMPT: ,END OF RAY TEST, HTABLES[I]
+ L → H00 + COUNT → H01, HTABLES [I+1] + L → H10 + COUNT →
H11, NTABLES [I] + L → N00 + COUNT → N01, NTABLES[I+1] + L →
N10 + COUNT → N11. |X[I+1] - X[I]| → DELTAX,

```

```
CMPT:
```

```

A[N01] - A[N00] → TS, (((A[N11] - A[N10] - TS) * (RANGE[1] +
XPRIME)) / DELTAX) + TS → TS, A[H01] - A[H00] → TS1,
(((A[H11] - A[H10] - TS1) * (RANGE[1] + XPRIME)) / DELTAX) +
TS1 → TS1, (TS/TS1) * DELTAH → DELTAN, (B*B) / 2.0 + (0.048 *
DELTAH) + DELTAN → BK< BKTEST:

```

```
, ONE HALF VALUES.;
```

```

, SQRT (BK;BK), (0.1339 * | DELTAH| ) / BK → XPRIME, HTESTS,
| (XPRIME - XPRIME[1]) * 100.0 | > XPRIME:

```

```
XPRIME → XPRIME[1], CMPT.;
```

```
CHANGE TABLES, END OF RAY TEST, 1.414213562 * BK → B,
```

```
PRINT OR PUNCH, 5 → J, ZERO LOCATIONS,
```

```
N = 1:
```

```
RESET;;
```

```
EXIT 4:} ..
```

5;

(:PAGE F4985-100n-7)

, ZERO LOCATIONS: {SW[J].

SW: ZERO ALL. EXIT. EXIT. EXIT. DHO.

EXIT.

ZERO ALL: 0 → PRINT H → PRINT H [1] → PRINT H [2] → I → J → K →  
 L → M → N → RANGE → RANGE [1] → RANGE [2], 5 → J, SW [J]. 0#0,  
 0#0, 0#0, 0#0, 0#0, 0#0, 0#0, 0#0, 0#0, 0#0, 0#0, 0#0, 0#0,  
 0#0, 0#0, 0#0, 0#0, 0#0, 0#0, 0#0, 0#0, DHO: 0 → DELTA H, EXIT.  
 EXIT: 0 → XPRIME → XPRIME[1] → XPRIME[2] → DELTAN → DELTAN [1]  
 → DELTAN [2] }

, PRINT OR PUNCH: { PRINTH + DELTAH → PRINTH, XPRIME + RANGE → RANGE,  
 XPRIME + RANGE[1] → RANGE[1],

PRINT TEST = 0:

XMAX ≥ 1000.0::

RANGE \* 10.0 → RANGE;

FLOAT PUNCH (RANGE, PRINTH, K;) K + 1 → K, XMAX ≥ 1000.0::

RANGE / 10.0 → RANGE;;

DELTAH → PRNTDH. {&lt;PRINTH| PRNTDH | B | XPRIME| DELTAN|RANGE&gt;;};

..

5;

(:PAGE F4985-100n-8)

,END OF RAY TEST: {PRINTH &lt; HMAX ∩ RANGE &lt; XMAX;;

SUBTRACT BS: BMAX - DELTAB → BMAX &lt; BMIN:

0 → RAY, END RUN #24, 0 #90, TF, STOP.

NEWRAY.;;}

,H IS ZERO: {PRINTH + DELTAH &gt; 0:

L + IORD → L;

REVERSE SIGNS, RESET PARAMETERS; }

CHANGE TABLES: {RANGE + X PRIME > X [I+1]:

5 → J, ZERO LOCATIONS,

|DELTA H/2.0| - |DELTA H MIN| < 0:

0 → RANGE [1], RESET PARAMETERS, RE.;

DELTA H/ 2.0 → DELTA H, CMPT.;

,ONE HALF VALUES: {5 → J , ZERO LOCATIONS,

| DELTAH / 2.0 | - | DELTAH MIN | < 0:

APPROXIMATION.;

BKTEST / 2.0 → BKTEST, DELTAH / 2.0 → DELTA H,

1 → N, M + COUNT → M,

ENTRY.} ..

5;

(:PAGE F4985-100n-9)

, HTESTS: { I OR D < 0:

MINUS.

PLUS.

MINUS: (((A[H10] - A[H00]) / DELTAX) \* (RANGE [1] + XPRIME))

+ A[H00] + DELTA H MIN → HO TEST,

L ≠ 0.;

HO TEST - DELTA H MIN → HO TEST;

PRINTH + DELTAH > HO TEST:

EXIT3.

PRINT H + DELTA H MIN < HO TEST:

,H IS ZERO, ST CMPT.;

EXIT2.

PLUS: (((A[H11] - A[H01]) / DELTAX) \* (RANGE[1] + XPRIME)) +

A[H01] + DELTA H MIN → H1 TEST,

PRINTH + DELTAH < H1 TEST:

EXIT3.

PRINT H + DELTA H MIN > H1 TEST:

L + IORD → L, ST CMPT.;

EXIT2.

EXIT2: 1 → N, DELTA H/2.0 → DELTA H, |DELTA H| \* BKM → BK TEST,  
START COMPUTE, 0 → M, ENTRY. EXIT3:{ ..

5;

(:PAGE F4985-100n-10)

, REVERSE SIGNS: {- DELTAH → DELTAH, - DELTAH[1] → DELTAH[1],  
- IORD → IORD, - B → B, - DELTAH MIN → DELTAH MIN, - DELTAH[3]  
→ DELTAH[3]}

, APPROXIMATION: {0 → N, IORD ≥ 0;;

- B → B;

- 3.959 \* B → XPRIME, ((XPRIME \* XPRIME)/ 7918.0 + ((B \*  
| XPRIME | ) \* 0.001)) \* 5280.0 → DELTAH[2], B → B[1], |XPRIME| →  
XPRIME, 0 → B, DELTAH → DELTAH[3], DELTAH[2] → DELTAH,

PRINT TEST = 0;;

, {<< ---- APPROXIMATION ---->>};

, PRINT OR PUNCH, B[1] → B, REVERSE SIGNS, PRINT OR PUNCH,  
DELTAH [3] → DELTAH, 5 → J, ZERO LOCATIONS, ENDOFRAYTEST,  
CHANGE TABLES, APPROX RE.} ..

5;

(:PAGE F4985-100n-11)

APPROX RE., START COMPUTE, RESET, M- COUNT → M, APPROX RE.

RESET: { |DELTAH[1]| - | DELTAH | < 0:

0 → N, RESET PARAMETERS, ENTRY.;

BKTEST \* 2.0 → BKTEST, DELTAH \* 2.0 → DELTAH, {

, RESET PARAMETERS: {BK TEST[1] → BK TEST, DELTA H[1] →  
DELTA H} ..

5;

(:PAGE F4985-100n-LAST)

TABLE ADDRESSES:

I = 1(1)99 {HTABLES[I-1] + #64 → HTABLES[I], NTABLES[I-1] + #64 →  
NTABLES[I],} 0 → I, #0C06 #10..

5

(:PAGE F4946B-1)

T|AB = #29,

F|LX.

C|R = #25.

C|T,

M|INUS = 11,

P|LUS = 10,

F|R.

F|LY.

X|Y;

FLOAT PUNCH (X. Y. LINE;):

{TAB #24, 0 #90, X → FLX, SPLIT (FLX; FLX, FR),

X < 0:

MINUS #24, 0 #90, -FLX → FLX;

PLUS #24, 0 #90;

|FR| > 0.5:

FLX + 1.0 → FLX;;

FL TO FX (FLX; XY),

XY = 10000:

XY -1 → XY;

XY = 10001:

XY -2 → XY;;;

CONVERT 1 (XY;),

(:PAGE F4946B-1)

Y → FLY, SPLIT (FLY; FLY, FR),

Y < 0:

MINUS #24, 0 #90, - FLY → FLY;

PLUS #24, 0 #90;

```

|FR| > 0.5:
  FLY + 1.0 → FLY;;
FL TO FX (FLY; XY),
XY = 10000:
  XY - 1 → XY;
  XY = 10001:
    XY - 2 → XY;;;
CONVERT 1 (XY;), CR #24, 0 #90}.

```

(:PAGE F4946B-3)

```

CONVERT 1 (XY;): {#10 → CT,
  T|HOUSAND:
    XY - 1000 → XY < 0:
      1000 + XY → XY, CT #24, 0 #90, #10 → CT, HUNDRED.
      CT + 1 → CT, THOUSAND.
  H|UNDRED:
    XY - 100 → XY < 0:
      100 + XY → XY, CT #24, 0 #90, #10 → CT, TENS.
      CT + 1 → CT, HUNDRED.
  T|ENS:
    XY - 10 → XY < 0:
      10 + XY → XY, CT #24, 0 #90, #10 → CT, UNITS.
      CT + 1 → CT, TENS.
  U|NITS:
    XY - 1 → XY < 0:
      CT #24, 0 #90, TAB #24, 0 #90;
      CT + 1 → CT, UNITS.}..

```

5

NR,

PRINTER OK,

RAY ;

RAY COUNTER (RAY;): { #10 → NR,

THOUS: RAY - 1000 → RAY < 0:

1000 + RAY → RAY, NR #24, 2 #90, #10 → NR, HUND.

NR + 1 → NR, THOUS.

HUND: RAY - 100 → RAY < 0:

100 + RAY → RAY, NR #24, 2 #90, #10 → NR, TEN.

NR + 1 → NR, HUND.

TEN: RAY - 10 → RAY < 0:

10 + RAY → RAY, NR #24, 2 #90, #10 → NR, ONES.

NR + 1 → NR, TEN.

ONES: RAY - 1 → RAY < 0:

NR # 24, 2 #90, #25 → [#3fff], #3fff #24, 2 #90;

NR + 1 → NR, ONES.

RAY + 1 → RAY{

..

5..

<b>DOCUMENT CONTROL DATA - R&amp;D</b>		
<i>(Security classification of title, body of abstract and indexing annotation must be entered when the overall report is classified)</i>		
1. ORIGINATING ACTIVITY <i>(Corporate author)</i> U.S. Naval Research Laboratory Washington, D.C. 20390		2a. REPORT SECURITY CLASSIFICATION <b>Unclassified</b>
		2b. GROUP
3. REPORT TITLE <b>RAY TRACING IN RISING AND FALLING DUCTS</b>		
4. DESCRIPTIVE NOTES <i>(Type of report and inclusive dates)</i> <b>A final report on one phase of the problem.</b>		
5. AUTHOR(S) <i>(Last name, first name, initial)</i> <b>Guinard, N.W., Laing, M.B., Morin, K.</b>		
6. REPORT DATE <b>June 22, 1965</b>	7a. TOTAL NO. OF PAGES <b>30</b>	7b. NO. OF REFS <b>4</b>
8a. CONTRACT OR GRANT NO. <b>NRL Problem R07-02</b>	9a. ORIGINATOR'S REPORT NUMBER(S) <b>NRL Report 6253</b>	
b. PROJECT NO. <b>RR 008-01-41-5550</b>	9b. OTHER REPORT NO(S) <i>(Any other numbers that may be assigned this report)</i>	
c.		
d.		
10. AVAILABILITY/LIMITATION NOTICES <b>Unlimited availability — Available at CFSTI</b>		
11. SUPPLEMENTARY NOTES	12. SPONSORING MILITARY ACTIVITY <b>Department of the Navy (Office of Naval Research)</b>	
13. ABSTRACT <p>In studying signal transmission beyond the horizon by elevated duct propagation, estimates are needed of the losses. These estimates can be made by application of ray tracing for models of longitudinally varying ducts. A program was written in the NELIAC language for producing ray trajectories in an atmosphere which is variable in two dimensions. The program was run in the NAREC digital computer, and the resulting plots of the ray paths are used to analyze certain of the loss mechanisms in elevated ducts. Changes of the acceptance angle, i.e., refractive index gradient at a fixed altitude can cause continued losses. Changes in duct geometry causes losses which are a function of the height slope distribution at the point of change. A third loss mechanism, that of scattering, is not handled in the present analysis, but it is pointed out that a discontinuous duct may approach the Booker and Gordon model for tropospheric scatter.</p>		

14. KEY WORDS	LINK A		LINK B		LINK C	
	ROLE	WT	ROLE	WT	ROLE	WT
Communication theory Wave transmission Radio communication systems Radio signals Radio transmission Programming (computers) Iterative methods Atmosphere Troposphere Ray tracing Duct geometry Elevated duct propagation Refractive index						

INSTRUCTIONS

1. **ORIGINATING ACTIVITY:** Enter the name and address of the contractor, subcontractor, grantee, Department of Defense activity or other organization (*corporate author*) issuing the report.
- 2a. **REPORT SECURITY CLASSIFICATION:** Enter the overall security classification of the report. Indicate whether "Restricted Data" is included. Marking is to be in accordance with appropriate security regulations.
- 2b. **GROUP:** Automatic downgrading is specified in DoD Directive 5200.10 and Armed Forces Industrial Manual. Enter the group number. Also, when applicable, show that optional markings have been used for Group 3 and Group 4 as authorized.
3. **REPORT TITLE:** Enter the complete report title in all capital letters. Titles in all cases should be unclassified. If a meaningful title cannot be selected without classification, show title classification in all capitals in parenthesis immediately following the title.
4. **DESCRIPTIVE NOTES:** If appropriate, enter the type of report, e.g., interim, progress, summary, annual, or final. Give the inclusive dates when a specific reporting period is covered.
5. **AUTHOR(S):** Enter the name(s) of author(s) as shown on or in the report. Enter last name, first name, middle initial. If military, show rank and branch of service. The name of the principal author is an absolute minimum requirement.
6. **REPORT DATE:** Enter the date of the report as day, month, year; or month, year. If more than one date appears on the report, use date of publication.
- 7a. **TOTAL NUMBER OF PAGES:** The total page count should follow normal pagination procedures, i.e., enter the number of pages containing information.
- 7b. **NUMBER OF REFERENCES:** Enter the total number of references cited in the report.
- 8a. **CONTRACT OR GRANT NUMBER:** If appropriate, enter the applicable number of the contract or grant under which the report was written.
- 8b, 8c, & 8d. **PROJECT NUMBER:** Enter the appropriate military department identification, such as project number, subproject number, system numbers, task number, etc.
- 9a. **ORIGINATOR'S REPORT NUMBER(S):** Enter the official report number by which the document will be identified and controlled by the originating activity. This number must be unique to this report.
- 9b. **OTHER REPORT NUMBER(S):** If the report has been assigned any other report numbers (*either by the originator or by the sponsor*), also enter this number(s).
10. **AVAILABILITY/LIMITATION NOTICES:** Enter any limitations on further dissemination of the report, other than those

imposed by security classification, using standard statements such as:

- (1) "Qualified requesters may obtain copies of this report from DDC."
- (2) "Foreign announcement and dissemination of this report by DDC is not authorized."
- (3) "U. S. Government agencies may obtain copies of this report directly from DDC. Other qualified DDC users shall request through \_\_\_\_\_."
- (4) "U. S. military agencies may obtain copies of this report directly from DDC. Other qualified users shall request through \_\_\_\_\_."
- (5) "All distribution of this report is controlled. Qualified DDC users shall request through \_\_\_\_\_."

If the report has been furnished to the Office of Technical Services, Department of Commerce, for sale to the public, indicate this fact and enter the price, if known.

11. **SUPPLEMENTARY NOTES:** Use for additional explanatory notes.
12. **SPONSORING MILITARY ACTIVITY:** Enter the name of the departmental project office or laboratory sponsoring (*paying for*) the research and development. Include address.
13. **ABSTRACT:** Enter an abstract giving a brief and factual summary of the document indicative of the report, even though it may also appear elsewhere in the body of the technical report. If additional space is required, a continuation sheet shall be attached.

It is highly desirable that the abstract of classified reports be unclassified. Each paragraph of the abstract shall end with an indication of the military security classification of the information in the paragraph, represented as (TS), (S), (C), or (U).

There is no limitation on the length of the abstract. However, the suggested length is from 150 to 225 words.

14. **KEY WORDS:** Key words are technically meaningful terms or short phrases that characterize a report and may be used as index entries for cataloging the report. Key words must be selected so that no security classification is required. Identifiers, such as equipment model designation, trade name, military project code name, geographic location, may be used as key words but will be followed by an indication of technical content. The assignment of links, roles, and weights is optional.